

# Modelling of Adaptive Neuro-Fuzzy Inference System (ANFIS) - Based Maximum Power Point Tracking (MPPT) Controller for a Solar Photovoltaic System

## Abstract :

**Aim:** The aim of this research is to model and simulate Adaptive Neuro-Fuzzy Inference System (ANFIS) based MPPT Controller and also compare its performance with the Perturb and Observe MPPT controller for Photovoltaic systems.

**Study of the design:** The PV system consists of a PV module, a PWM inverter, an MPPT controller and a DC-DC converter, all of which are connected using Matlab-Simulink environment

**Methodology:** The ANFIS reference model is constructed based on two input parameters: solar irradiance and temperature. Its output parameter is the reference maximum power output. The temperature and irradiance data employed for the particular site examined in this study have been acquired from an online global database. The P&O MPPT method was used as a benchmark against the proposed ANFIS-based MPPT technique using Matlab-Simulink Environment.

**Results:** In the absence of the controller, the PV voltage registered at 50V. However, through the ANFIS-based MPPT, the incoming voltage from the PV was able to roughly double. Conversely, in the absence of the controller, the PV current stabilized at 4.5A, but the ANFIS-based MPPT managed to reduce this incoming current from the PV by approximately half.

The generated PV power follows a similar trajectory to the theoretical PV power, reaching a peak of around 420W, which closely aligns with the theoretical peak power of 440W. The

power spans the range from nearly 0 to 420W. As a result, the overall efficiency of the ANFIS-based MPPT charge controller is estimated to be around 60%.

**Conclusion:** The evaluation of the ANFIS-based MPPT and Perturb and Observe-based MPPT Controllers reveals that the Perturb and Observe-based controller demonstrated superior efficiency. Based on this investigation, it can be inferred that both MPPT controllers effectively address uncertain weather scenarios and can readily accommodate challenges such as partial shading and other irregularities commonly associated with varying weather conditions.

Keywords: efficiency, weather, adaptive, model, simulate

## 1. INTRODUCTION

Electric energy constitutes the essential power requirement for sustaining human life, particularly in fulfilling fundamental necessities such as food, shelter, and clothing. Electricity consumption primarily stems from fossil fuels, with the remaining portion sourced from renewable energy outlets. The utilization of fossil fuels has given rise to a host of predicaments encompassing environmental, health, and economic realms. Among the assortment of renewable energy resources, solar energy takes precedence. Solar energy is comprised of heat and light radiated by the sun, a vast energy reservoir that emits an immense quantity of energy toward the Earth's surface. The terrestrial surface is bestowed with an influx of solar energy reaching up to 1,000 watts per square meter [1].

An Adaptive Neuro-Fuzzy Inference System (ANFIS) is a type of artificial intelligence model that combines the principles of fuzzy logic and neural networks to create a powerful system capable of handling complex and uncertain data. ANFIS is particularly well-suited for systems that require decision-making and control based on input parameters that might not be precisely defined. A charge controller is a device used in photovoltaic (solar power) systems

to regulate the charging process of batteries. Its primary function is to ensure that the batteries are charged efficiently, prevent overcharging, and extend the battery lifespan.

The global rise in energy demand fosters the need for alternative energy sources, this has prompted the urgent need for concept of maximum power point tracking as an essential technology for improving the efficiency of PV modules. It is evident that the use of solar modules without MPPT controllers results in energy wastages, which ultimately results in the need to install more PV modules for the same power requirement. Several MPPT controllers have been designed, but they have not been able to address the deficit in efficiency of PV modules which might have resulted from dependence of solar photovoltaic modules on irradiance and temperature for the power generation, these two factors vary with varying atmospheric conditions like weather, climate, and seasons. Other conditions like partial shading due to cloud cover, nearby trees, buildings, and dust also have adverse effects on PV-based power generation; it has become important to design an improved MPPT controller for highly efficient PV-based power generation.

Due to diverse developmental activities, there has been a rise in global energy requirements across all sectors. As reliance on fossil fuel-centered technology diminishes rapidly, the moment has arrived to tap into alternative energy sources like solar, wind, biomass, and small-scale hydropower in order to address the energy challenge [2].

In essence, the Maximum Power Point Tracking (MPPT) controller is composed of a DC–DC power converter that functions through an algorithm aimed at optimizing the solar panel's output to align with the Maximum Power Point (MPP).

The strategies employed to achieve Maximum Power Point Tracking (MPPT) can be classified into two main categories: traditional techniques which include incremental conductance (InCon) [3,4], open-circuit voltage (OCV) method [5,6] and the perturbation and observation (P&O) [7–9]; and artificial intelligence (AI) methods like artificial neural

networks (ANN) [10], fuzzy logic (FL) [11], particle swarm optimization (PSO) [12], and adaptive neuro-fuzzy inference system (ANFIS) [13].

P&O and InCon are conventionally favored MPPT strategies due to their straightforward hardware configuration, minimal sensor prerequisites, and cost-effectiveness. Nonetheless, as documented in references [14–16], these conventional methodologies encounter various challenges. These include sluggish tracking speed, significant fluctuations centered around the MPP, and instability during swift shifts in weather conditions. Furthermore, these conventional methods are fine-tuned for consistent environmental scenarios and might encounter difficulty in precisely tracing the global maximum power point (GMPP) under nonlinear and partially shaded conditions [17].

Recent progress has ushered in AI-based MPPT techniques to address the predicaments linked to conventional methods. Amid these, the FL-based MPPT controller emerges for its swift tracking pace and reduced oscillations, as substantiated by sources [18–19]. Nevertheless, the efficacy of this technique heavily hinges on a comprehensive comprehension of PV systems. Consequently, the proficiency of the FL-based controller strongly rests upon the meticulous design of fuzzy rules and membership functions.

Similarly, the ANN-based MPPT controller offers itself as a resilient approach, adept at handling intricate and nonlinear functions. Nonetheless, these controllers are accompanied by certain constraints, encompassing the requirement for a substantial volume of training data to ensure precision, extended training durations, and the intricacies linked to the design of ANN architectures. In order to proffer solutions to these challenges and limitations, Fuzzy Logic can be efficiently combined with Artificial Neural Network (ANN) to derive **an** ANFIS-based MPPT controller. **In** this study, the modelling and simulation of ANFIS-based MPPT controller and Perturb and Observe (PO) based MPPT controller in Matlab-Simulink

environment are critically evaluated, and their performance in terms of efficiency is compared.

## 2.0 Adaptive Neuro- Fuzzy Inference System

The Adaptive Neuro-Fuzzy Inference System (ANFIS) embodies a data learning approach that utilizes Fuzzy Logic (FL) to transform system input signals into precise outputs. This technique involves employing intricately interconnected artificial neural networks, with the neural connections carrying designated weights to faithfully convert numerical inputs into the desired output outcomes [20]. Through the amalgamation of strengths found in both machine learning methodologies, ANFIS presents a harmonized synthesis of capabilities derived from these two distinct techniques. To showcase the ANFIS architecture, we consider two fuzzy IF-THEN rules based on a first-order Sugeno model [21].

Rule 1 = If  $x$  is  $A_1$  and  $y$  is  $B_1$  Then  $f_1 = p_1x + q_1y + r_1$

Rule 2 = If  $x$  is  $A_2$  and  $y$  is  $B_2$  Then  $f_2 = p_2x + q_2y + r_2$

$A_1, A_2, B_1,$  and  $B_2$  represent the membership functions for each input  $x$  and  $y$ , forming part of the premises. The linear parameters  $p_1, q_1, r_1,$  and  $p_2, q_2, r_2$  pertain to the consequent section of the Takagi–Sugeno fuzzy inference model. With reference to Figure 1, the ANFIS architecture comprises five layers. The first and fourth layers feature adaptive nodes, while the remaining layers house fixed nodes. A concise description of each layer follows:

Layer 1: Each node in this layer adjusts to a function parameter. The output produced by each node is a degree of membership value, obtained from the input of the membership function.

As an illustration, the membership function could take the form of a Gaussian membership function (as shown in Equation 1), a generalized bell membership function (as demonstrated in Equation 2), or any other variety of membership function.

$$\mu_{A_i}(x) = \exp\left[-\left(\frac{x-c_i}{2a_i}\right)^2\right] \quad (1)$$

$$\mu_{A_i}(x) = \frac{1}{1 + \left| \frac{x - c_i}{a_i} \right|^{2b}} \quad (2)$$

$$O_{1,i} = \mu_{A_i}(x), \quad i = 1, 2 \quad (3)$$

$$O_{1,i} = \mu_{B_{i-2}}(y), \quad i = 3, 4 \quad (4)$$

In this context,  $\mu_{A_i}$  and  $\mu_{B_{i-2}}$  denote the degree of membership functions associated with the fuzzy sets  $A_i$  and  $B_i$  respectively. The parameters  $\{a_i, b_i, c_i\}$  determine the membership function's characteristics, allowing for the alteration of its shape. These parameters within this layer are typically termed as premise parameters.

Layer 2: Within this layer, all nodes remain static and non-adaptive, and the circular node is denoted as "II." The output node reflects the result of the incoming signal to the node, which is then passed on to the subsequent node through multiplication. Each node in this layer represents the strength of activation for a specific rule. In this second layer, the T-norm operator, often exemplified by the AND operator, is utilized to produce the output.

$$O_{2i} = w_i = \mu_{A_i}(x) * \mu_{B_i}(y), \quad i = 1, 2 \quad (5)$$

Regarding  $w_i$ , it serves as the output indicative of the firing intensity for each rule.

Layer 3: Within this layer, all nodes remain constant and non-adaptive, and the circular node is identified as "N." Each node calculates the ratio between the firing strength of the  $i$ -th rule and the aggregate firing strengths of all the rules. This outcome is termed the normalized firing strength.

$$O_{3,i} = \bar{w}_i = \frac{w_i}{w_1 + w_2}, \quad i = 1, 2 \quad (6)$$

Layer 4 comprises exclusively of adaptive nodes, each associated with an output, where a node is explicitly characterized by its definition as

$$O_{4i} = \bar{w}_i f_i = \bar{w}_i (p_i x + q_i y + r_i) \quad (7)$$

$\bar{w}_i$  represents the standardized firing potency derived from the preceding layer (referred to as the third layer), while  $(p_i x + q_i y + r_i)$  denotes a parameter within the node. The attributes within this stratum are recognized as subsequent parameters.

Layer 5: Within this tier, a solitary node exists, which is stationary and not subject to adaptability. It computes the ultimate output by aggregating all inbound signals originating from the antecedent node. In this layer, the circular node is designated as  $\Sigma$ .

$$O_{5i} = \sum_i \bar{w}_i f_i = \frac{\sum_i w_i f_i}{\sum_i w_i} \quad (8)$$

ANFIS, recognized as an adaptive neural fuzzy logic network, mimics the behaviors exhibited by neural and fuzzy inference systems. In the adaptive neural network, synaptic weights remain absent, but a combination of non-adaptive and adaptive nodes exists within its framework. It is readily transformed into a neural network structure employing a conventional feedforward topology, thus earning it the label of an adaptive network [22].

The configuration of the ANFIS adaptive network bears a resemblance to an emulator for the adaptive Takagi–Sugeno's fuzzy controllers. The operational characteristics of this adaptive network closely parallel those of a fuzzy inference system (FIS).

Input and output parameters of the ANFIS network are fine-tuned through the utilization of back-propagation gradient descent and the least-squares technique applied to the provided input/output dataset. These parameters, both linear and nonlinear, are fundamental components of the network. The ANFIS network consists of two primary sections: the antecedent part and the consequent part. These segments are interlinked via a rule-based system inherent to the fuzzy inference system. The structure of the ANFIS with five layers is depicted in Figure 1.

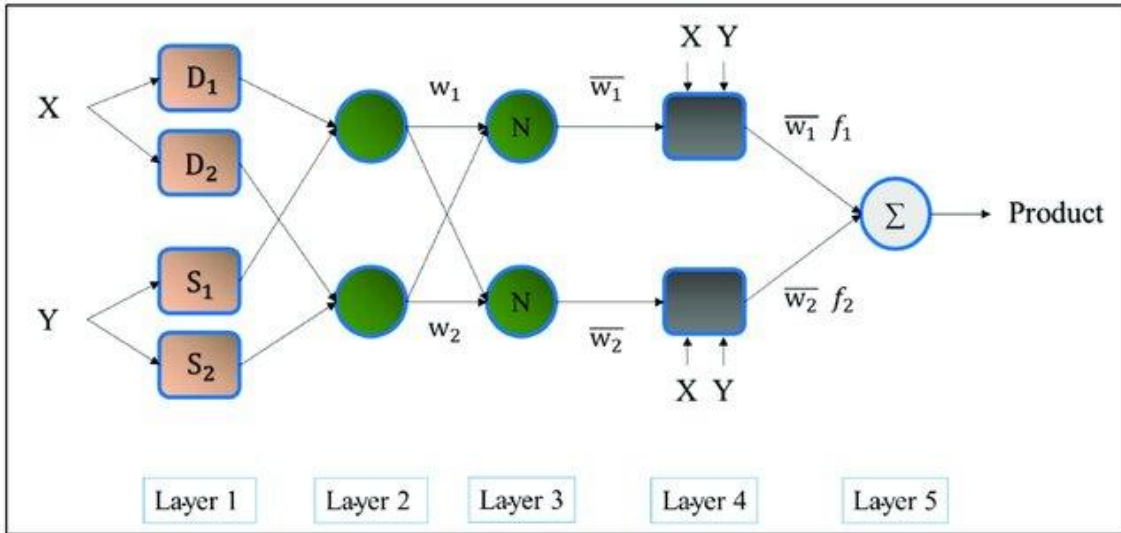


**Figure 1: Structure of ANFIS with layers.[23]**

### 3.0 METHODOLOGY

#### 3.1 Solar Photovoltaic System Modelling

In this research work, the PV system consists of a PV module, PWM inverter, MPPT controller and DC-DC converter. The ANFIS based MPPT and PO based MPPT controller defines the duty cycle (D) that is supplied to the DC-DC converter which it uses for adjusting the current and voltage.

#### Mathematical modelling of a Photovoltaic module

Through the PV effect, radiation from the solar energy is transformed to electricity, as the sun intensity increases, photons with energy higher than band gap energy of the semiconductor makes electron-hole pairs that is proportional to the incident radiation. Figure 2 shows the equivalent circuit of a PV cell.

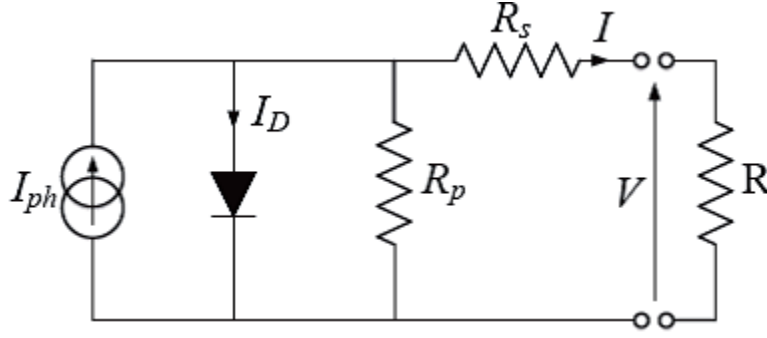


**Figure 2: Equivalent circuit of a PV cell**

As shown the figure above,  $I_{ph}$  represents the cell photocurrent,  $R_{sh}$  represents the cell's shunt resistances, while  $R_s$  represents the cell's series resistances. When PV cells are grouped together, they are regarded as PV modules, and they can be further interconnected in a parallel-series configuration to form PV arrays. In Equations (9) to (12), the mathematical model equations for photovoltaic panel are described [24] [25]

For module photocurrent,

$$I_{ph} = [I_{scr} + K_i(T - 298)] * \lambda/1000 \quad (9)$$

For module reverse saturation current,

$$I_{rs} = I_{scr} / [\exp(q \cdot \frac{V_{oc}}{N_s} \cdot k \cdot A \cdot T)] \quad (10)$$

Module saturation current  $I_s$  varies according to cell temperature, given as:

$$I_s = I_{rs} * \left[ \frac{T}{T_r} \right] * 3 * \exp \left[ q * E_{go} \left( \left( \frac{1}{T_r} \right) - \left( \frac{1}{T} \right) \right) \right] \quad (11)$$

The PV module current is given as:

$$I_{pv} = N_p * I_{ph} - N_p * I_s \left[ \exp \left( \frac{q * V_{pv} + I_{pv} * R_s}{N_s A k T} \right) \right] \quad (12)$$

Where,  $V_{PV} = V_{OC}$ ,  $N_P = 2$ ,  $N_S = 2$

From the above equations,  $V_{PV}$  represents PV module output voltage,  $V_{OC}$  represents open circuit voltage,  $I_{pv}$  represents PV module output current,  $T_r$  represents the reference temperature,  $I_{ph}$  represents light-generated current,  $I_s$  represents PV module saturation current(A),  $A$  is the ideality factor which is 1.6,  $K$  represents the Boltzman constant ( $1.3805 \times$

$10^{-23}$  J/K),  $q$  is the electron charge ( $1.6 \times 10^{-19}$  C),  $R_s$  represents PV module series resistance,  $I_{scr}$  represents PV module short circuit current,  $K_i$  represents short-circuit current temperature coefficient ( $I_{scr} = 0.0017 \text{ A/}^\circ\text{C}$ ),  $\lambda$  represents PV module illumination ( $\text{W/m}^2$ ),  $E_{go}$  represents band gap for silicon (1.1 eV),  $N_s$  represents the number of cells connected in series,  $N_p$  represents the number of cells connected in parallel.

In this research work, solar PV array (1Soltech 1STH- 215-P) was selected for the proposed model in matlab/simulink, The specifications of the PV module connected DC-DC converter and battery is shown in Table 1 and Figure 3, the PV array consists of 2 (two) PV modules connected in series. Figure 4 - 5 shows the changes in I-V and P-V output with respect to irradiation and temperature. Figure 3 shows the changes in current and power at different radiations under a specific temperature of  $25^\circ\text{C}$ ; Figure 4 shows the changes in current and power at different temperatures under specific radiation of  $1000 \text{ W/m}^2$ .

**Table 1: Data specifications for the PV system**

PV Module		DC-DC converter	
Parameter	Value	Parameter	Value
$P_{max}$ (W)	213.5	Output Capacitor (farad)	100e-6
$V_{oc}$ (V)	36.3	Inductance(H)	2e-3
$I_{sc}$ (A)	7.84	Input capacitor (farad)	100e-4
$V_{mp}$ (V)	29	Switch frequency (KHz)	5
$I_{mp}$ (A)	7.35		

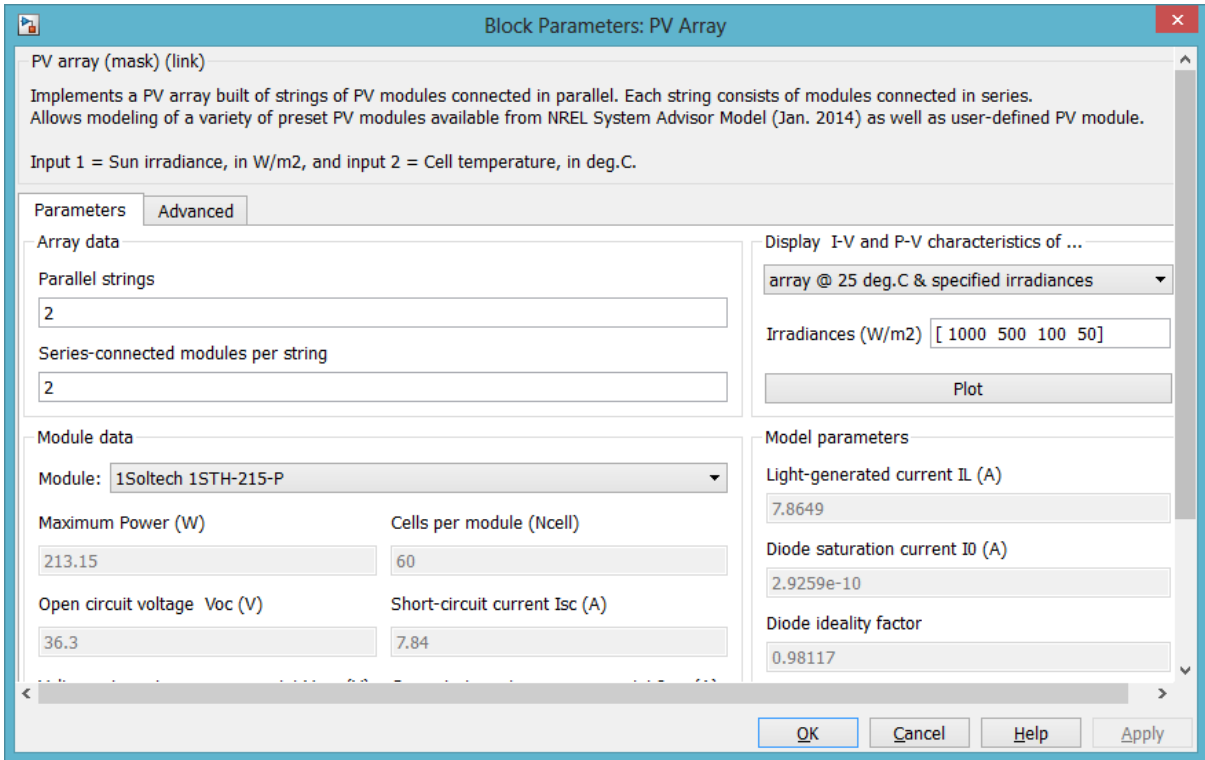


**Figure 3: Design specification for PV module**

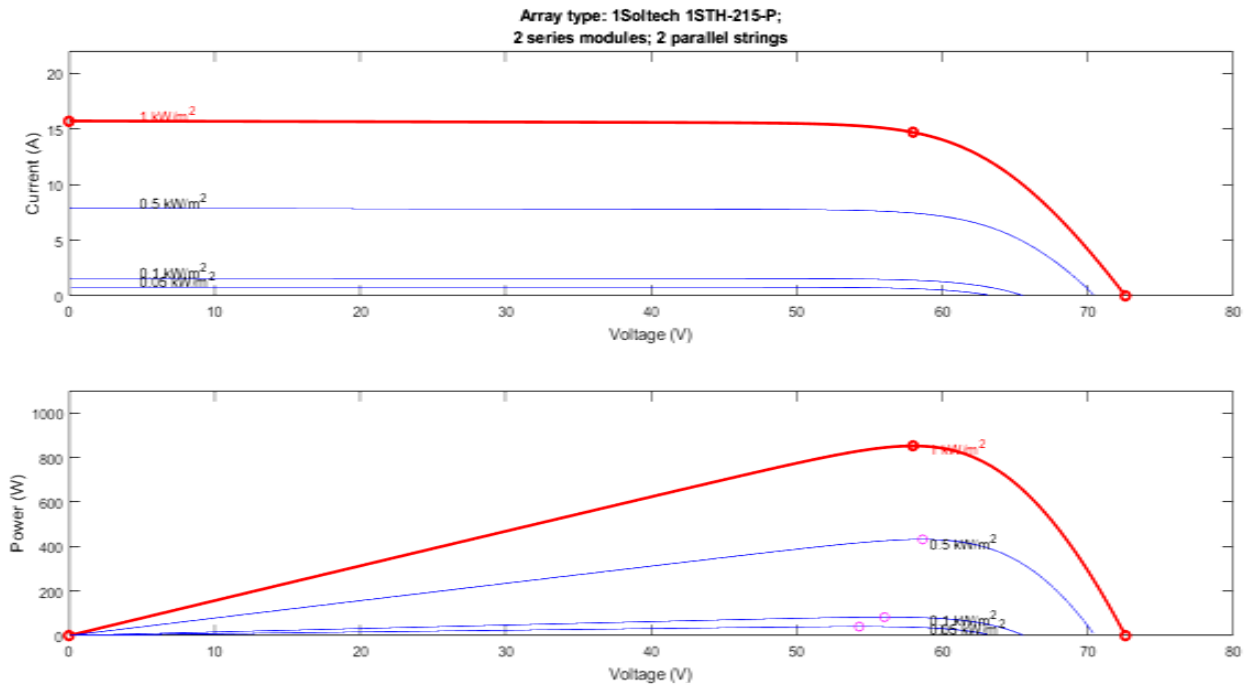


**Figure 4: Current and Power variation at different radiation under specific temperature of 25°C**

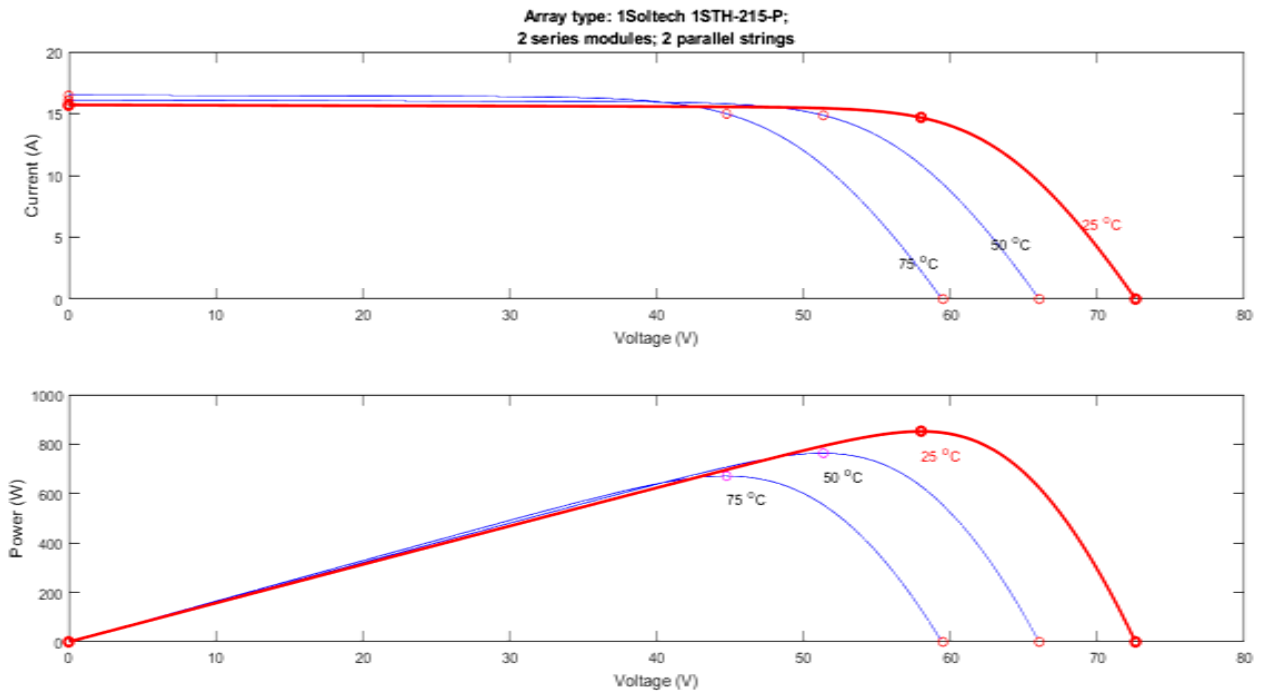


**Figure 5: Current and Power variation at different temperatures under specific irradiation of  $1000\text{W}/\text{m}^2$**

### **3.2 ANFIS-Based MPPT Controller**

The ANFIS reference model is built upon a foundation of two input variables: solar irradiance and temperature. Its output variable is the reference maximum power output. The temperature and irradiance values utilized for the specific site under investigation in this research have been sourced from the online global database. Figure 6 shows the ANFIS architecture with seven membership functions for solar irradiance and seven membership functions for temperature.

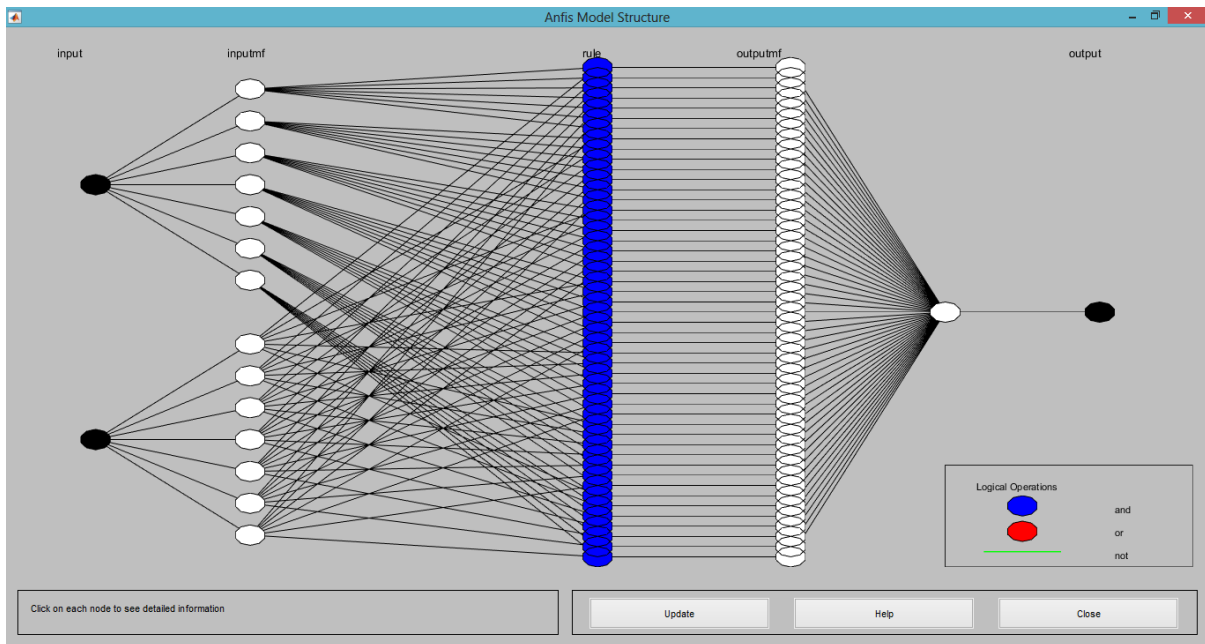


**Figure 6: ANFIS Architecture**

### 3.2.1 ANFIS Controller training with the Solar Parameters

The dataset used for the training procedure includes two input parameters: irradiance and temperature, and a single output parameter: either PV panel voltage, PV panel current, or PV panel power. The initial step in training the ANFIS controller within MATLAB involves loading the input and output data of the PV array. Once the data is loaded, membership functions for the inputs were defined using the grid partition method through subtractive clustering. To facilitate training, a hybrid learning algorithm is applied to the ANFIS controller, with a total of 1000 iterations for the training process. Subsequently, the ANFIS controller is subjected to testing using independent testing data. Upon successful testing and validation of the ANFIS controller, it is further transformed into a reference PV model.

Figure 7 shows the training process of the ANFIS controller in MATLAB

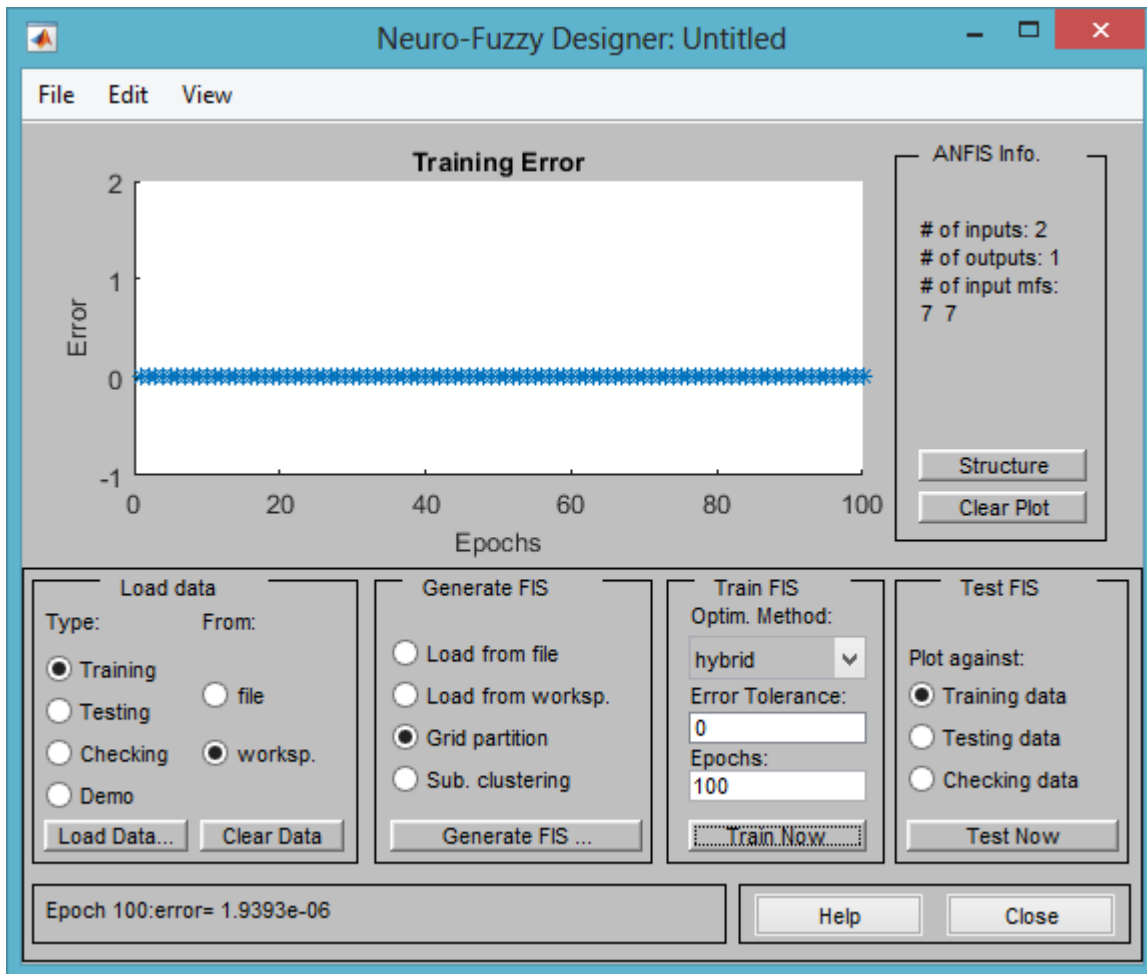


**Figure 7: Training process for the ANFIS controller**

Upon the completion of ANFIS controller training, it is seamlessly integrated into the Simulink model for further analysis and evaluation.

### 3.3 Design of the Perturbation and Observation MPPT Controller.

The P&O MPPT approach stands as a widely adopted technique to enhance the efficiency of solar photovoltaic (SPV) modules. This method involves initially introducing a small change to the operational voltage of the PV module. Subsequently, the resulting power output of the PV module is computed and contrasted with its previous output. The disparity between these two power outputs (referred to as  $\Delta P$ ) is determined. If  $\Delta P$  is found to be positive, the perturbation is maintained in that direction. However, if  $\Delta P$  becomes negative, the perturbation direction is reversed. This iterative process is reiterated until the maximum power point (MPP) is attained. Within the context of this paper, the P&O MPPT method

serves as a benchmark against the proposed ANFIS-based MPPT technique. Further elaboration on the P&O MPPT technique can be found in references [26 - 32].

#### 4. Results and Discussion

The Simulink model (Figure 8) developed was subjected to testing under varying levels of solar irradiation and temperature. Signal builder block in the simulink model inputs varying signals to the PV module, these includes various weather conditions that affects performance of charge controller. The irradiance level distribution is shown in Fig. 9, solar radiation continuously changes within a time sequence, the maximum irradiance and temperature noticed is approximately  $600\text{W/m}^2$  and  $26^\circ\text{C}$  (Fig. 10) respectively which occurs during the noon of the day.

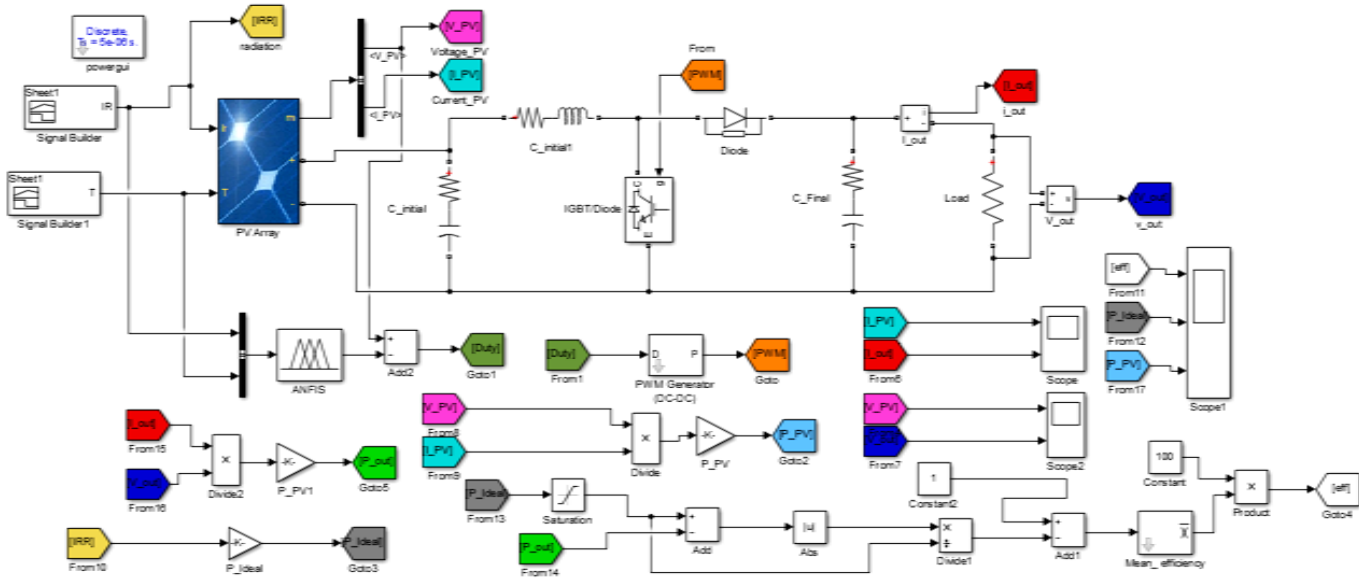
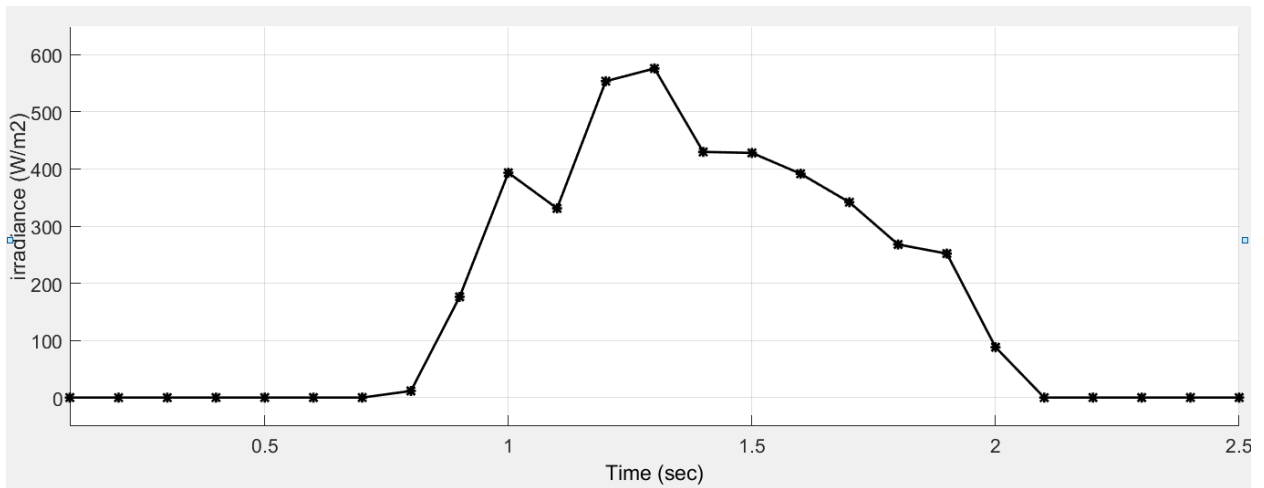
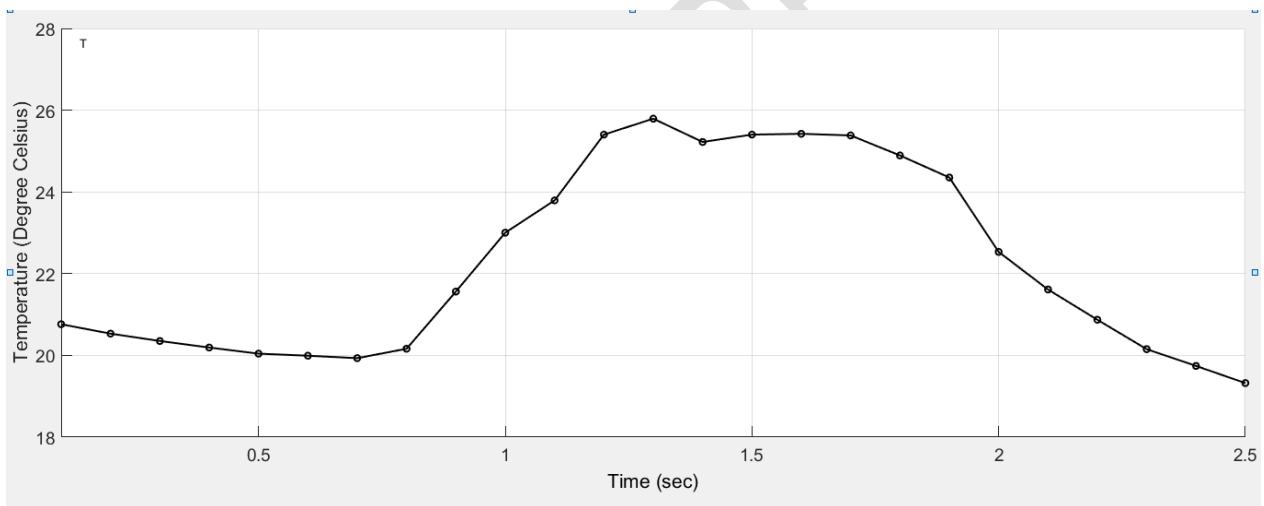


Figure 8: Simulink model for ANFIS based MPPT Charge Controller



**Figure 9 : Solar Radiation Profile obtained from a Site**



**Figure 10 : Temperature Profile obtained from a Site**

Within this Simulink model, several components are present, including a PV array, a PWM inverter and an MPPT controller. The meticulously developed Simulink model undergoes testing employing two distinct controllers for maximum power point tracking. These controllers encompass techniques such as Perturb and Observe (PO) and Adapted Neuro

fuzzy Inference System (ANFIS). The performance evaluation of the developed Simulink model is carried out under **two** different operational scenarios, which encompass conditions of steady-state irradiance and temperature, among others.

The ANFIS based MPPT controller is simulated at varying temperature and irradiance **levels** and then compared with the simulation of PV without the influence of the controller. Figure 11 shows PV voltage output with the ANFIS based MPPT (black line) and without the controller (blue line). In Figure 11, the PV voltage rises sharply from zero up to maximum voltage of 80V after a time of 1.25 **seconds**, **representing** the time of the day when peak solar radiation is experienced. For the system without the controller (Fig. 11), **a** PV voltage of 50V was **observed**; therefore the ANFIS based MPPT was able to approximately double the incoming voltage from the PV. The PV current decreases sharply from 9A to 4.5A after a time of 1.25**seconds**. **In** the system without the controller, the PV current of 4.5A was **observed**; therefore the ANFIS based MPPT was able to approximately decrease to half of the incoming current from the PV. Figure 12 shows the relationship between the ideal PV power and the generated PV power, the PV power generated shows similar trend with the ideal PV power, the peak value of PV power is about 420Watt which is close to the peak ideal power of 440Watt. **The** power changes from about 0 to 420Watt, **and** the overall efficiency of ANFIS based MPPT charge controller is approximately 60%.

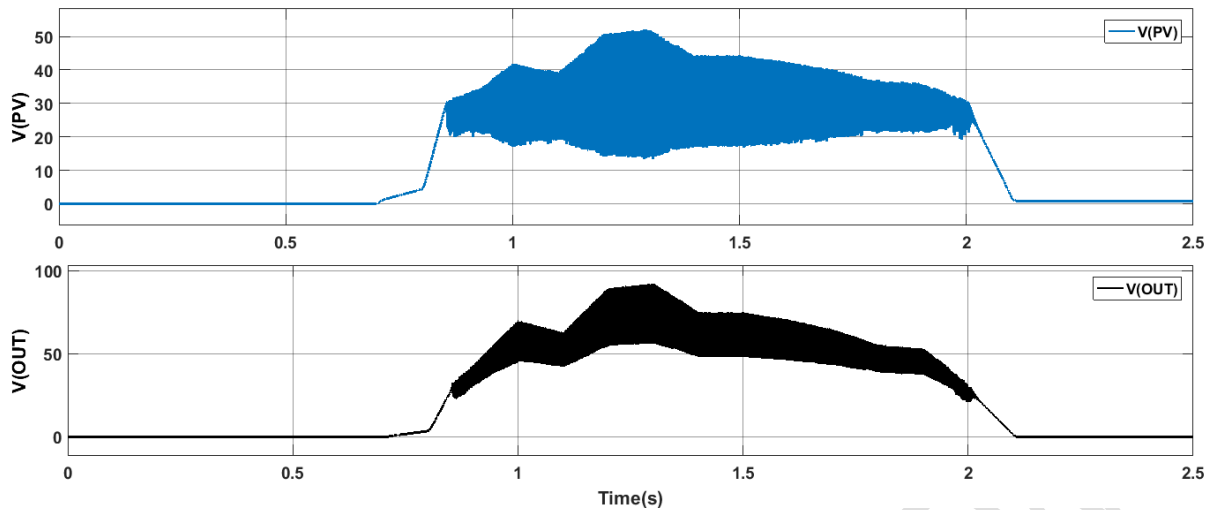


**Figure 11: PV and Converter Voltage Profile for ANFIS based MPPT Controller**

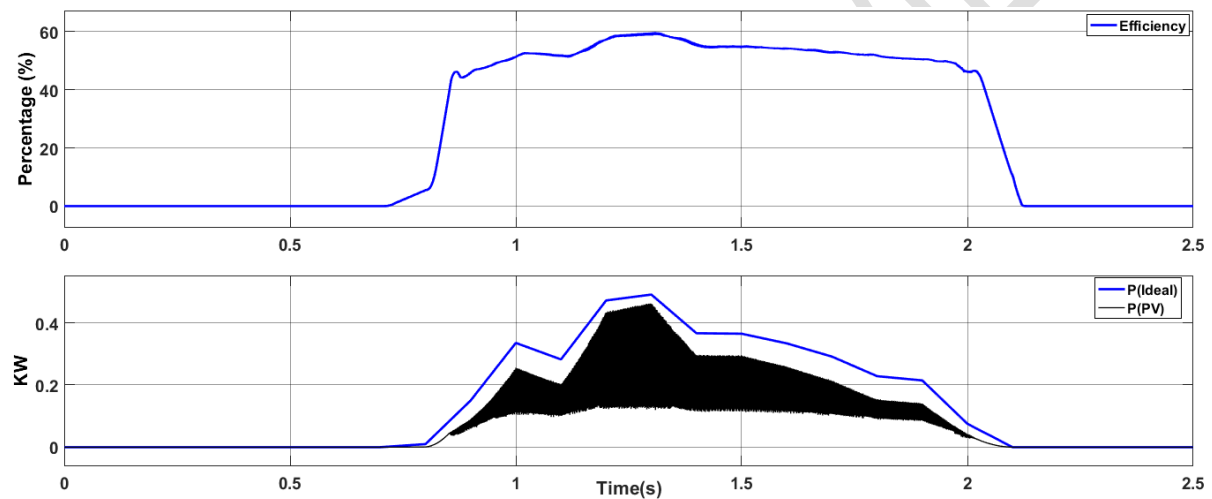


**Figure 12: Efficiency and PV Power Profile for ANFIS based MPPT Controller**

The Perturb and Observe (PO) based MPPT controller is simulated at varying temperature and irradiance, and then compared with the simulation of PV without the influence of the controller. Figure 13 shows the PV module voltage output with the ANFIS based MPPT (black line) and without the controller (blue line). In Figure 13, the PV voltage rises sharply from zero up to maximum voltage of 80V after a time of 1.25s which represents the time of the day when peak solar radiation is experienced. For the system without the controller (Fig. 5), the PV voltage of 50V was observed, Therefore, the ANFIS based MPPT was able to approximately double the incoming voltage from the PV. The PV current decreases sharply from 9A to 4.5A after a time of 1.25s. In the system without the controller, the PV current of

4.5A was noticed, therefore the ANFIS based MPPT was able to approximately decrease to half of the incoming current from the PV. Figure 14 shows the relationship between the ideal PV power and the generated PV power, the PV power generated shows similar trend with the ideal PV power. The peak value of PV power is about 420Watt, which is close to the peak ideal power of 440Watt, the power changes from about 0 to 420Watt, the overall efficiency of ANFIS based MPPT charge controller is approximately 99%.

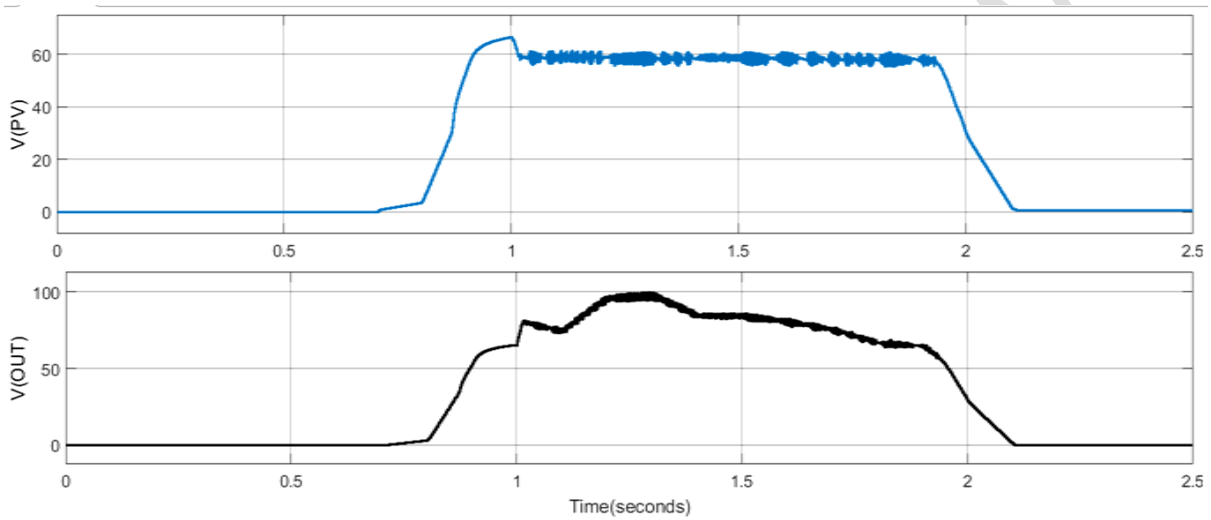


**Figure 13: PV and Converter Voltage Profile for PO based MPPT Controller**

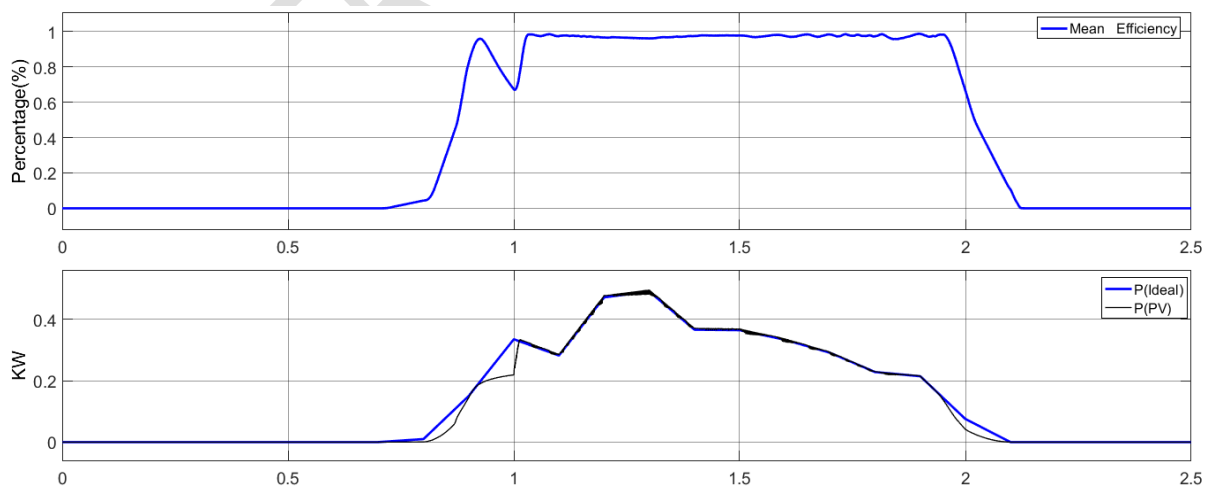


**Figure 14: Efficiency and PV Power Profile for PO based MPPT Controller**

## 6. Conclusion

The comparison of the performance of ANFIS based MPPT and Perturb and Observe based MPPT Controller shows that the Perturb and Observe based MPPT controller exhibited higher efficiency and is also characterized by a closer power output to the ideal power supplied by a typical MPPT controller. This study concludes that both MPPT controllers are effective for uncertain weather conditions and can be easily adapted for partial shading and other irregularities associated with weather conditions.

## References

- [1] Sharma, R., Goel, S. and Lenka, S.R. (2023). Pragmatic analysis of solar photovoltaic system design in an institutional building in eastern India. *Front. Energy Res.* 11:943207. doi: 10.3389/fenrg.2023.943207.
- [2] S. R. Revathy, V. Kirubakaran, M. Rajeshwaran, T. Balasundaram, V. S. Chandra Sekar, Saad Alghamdi, Bodour S. Rajab, Ahmad O. Babalghith, and Endalkachew Mergia Anbesse (2022). Design and Analysis of ANFIS – Based MPPT Method for Solar Photovoltaic Applications, Hindawi, *International Journal of Photoenergy*, Article ID: 9625564, 9 pages <https://doi.org/10.1155/2022/9625564>
- [3] Putri, R. I., Wibowo, S., and Rifa'i, M., 2015, "Maximum Power Point Tracking for Photovoltaic Using Incremental Conductance Method," *Energy Procedia*, 68, pp. 22–30.

- [4] Safari, A., and Mekhilef, S., 2011, "Incremental Conductance MPPT Method for PV Systems," 24th Canadian Conference on Electrical and Computer Engineering (CCECE), Niagara Falls, ON, Canada, May 8–11, pp. 000345–000347.
- [5] Das, P., 2016, "Maximum Power Tracking Based Open Circuit Voltage Method for PV System," Energy Procedia, 90, pp. 2–13.
- [6] Ch, S. B., Kumari, J., and Kullayappa, T., 2011, "Design and Analysis of Open Circuit Voltage Based Maximum Power Point Tracking for Photovoltaic System," Int. J. Adv. Sci. Technol., 2, pp. 51–60.
- [7] Dzung, P. Q., Le Dinh, K., Hong Hee, L., Le Minh, P., and Nguyen Truong Dan, V., 2010, "The New MPPT Algorithm Using ANN-Based PV," International Forum on Strategic Technology, Ulsan, South Korea, Oct. 13–15, pp. 402–407.
- [8] Mahamudul, H., Saad, M., and Ibrahim Henk, M., 2013, "Photovoltaic System Modeling With Fuzzy Logic Based Maximum Power Point Tracking Algorithm," Int. J. Photoenergy, 2013, p. 762946.
- [9] Liu, Y., Huang, S., Huang, J., and Liang, W., 2012, "A Particle Swarm Optimization-Based Maximum Power Point Tracking Algorithm for PV Systems Operating Under Partially Shaded Conditions," IEEE Trans. Energy Convers., 27(4), pp. 1027–1035.
- [10] Dzung, P. Q., Le Dinh, K., Hong Hee, L., Le Minh, P., and Nguyen Truong Dan, V., 2010, "The New MPPT Algorithm Using ANN-Based PV," International Forum on Strategic Technology, Ulsan, South Korea, Oct. 13–15, pp. 402–407.
- [11] Mahamudul, H., Saad, M., and Ibrahim Henk, M., 2013, "Photovoltaic System Modeling With Fuzzy Logic Based Maximum Power Point Tracking Algorithm," Int. J. Photoenergy, 2013, p. 762946.

- [12] Liu, Y., Huang, S., Huang, J., and Liang, W., 2012, "A Particle Swarm Optimization-Based Maximum Power Point Tracking Algorithm for PV Systems Operating Under Partially Shaded Conditions," *IEEE Trans. Energy Convers.*, 27(4), pp. 1027–1035.
- [13] Aldair, A. A., Obed, A. A., and Halihal, A. F., 2018, "Design and Implementation of ANFIS-Reference Model Controller Based MPPT Using FPGA for Photovoltaic System," *Renew. Sustain. Energy Rev.*, 82, pp. 2202–2217.
- [14] Lyden, S., and Haque, M. E., 2015, "Maximum Power Point Tracking Techniques for Photovoltaic Systems: A Comprehensive Review and Comparative Analysis," *Renew. Sustain. Energy Rev.*, 52, pp. 1504–1518.
- [15] Ben Salah, C., and Ouali, M., 2011, "Comparison of Fuzzy Logic and Neural Network in Maximum Power Point Tracker for PV Systems," *Electric Power Syst. Res.*, 81(1), pp. 43–50.
- [16] Gupta, A., Kumar, P., Pachauri, R. K., and Chauhan, Y. K., 2014, "Performance Analysis of Neural Network and Fuzzy Logic Based MPPT Techniques for Solar PV Systems," 2014 6th IEEE Power India International Conference (PIICON), Delhi, India, Dec. 5–7, IEEE, pp. 1–6.
- [17] Chim, C. S., Neelakantan, P., Yoong, H. P., and Teo, K. T. K., 2011, "Fuzzy Logic Based MPPT for Photovoltaic Modules Influenced by Solar Irradiation and Cell Temperature," 2011 UkSim 13th International Conference on Computer Modelling and Simulation, Cambridge, UK, Mar. 30–Apr. 1, IEEE, pp. 376–381.
- [18] Menniti, D., Pinnarelli, A., and Brusco, G., 2011, "Implementation of a Novel Fuzzy-Logic Based MPPT for Grid-Connected Photovoltaic Generation System," 2011 IEEE Trondheim PowerTech, Trondheim, Norway, June 19–23, IEEE, pp. 1–7.

- [19] Jiang, L. L., Nayanisiri, D. R., Maskell, D. L., and Vilathgamuwa, D. M., 2015, "A Hybrid Maximum Power Point Tracking for Partially Shaded Photovoltaic Systems in the Tropics," *Renew. Energy*, 76, pp. 53–65.
- [20] Ranganai, T. M., Pavel Y. T., Sibusiso. M. (2021). Design and Modeling of the ANFIS-Based MPPT Controller for a Solar Photovoltaic System. *Journal of Solar Energy Engineering*. AUGUST 2021, Vol. 143 / 041002-1
- [21] Suparta, W., Alhasa, K.M (2013) A comparison of ANFIS and MLP models for the prediction of precipitable water vapor. 2013 IEEE international conference on space science and communication (IconSpace), pp 243–248
- [22] A. A. Hepzibah, K. Premkumar. (2019). ANFIS current–voltage controlled MPPT algorithm for solar powered brushless DC motor based water pump. *Electrical Engineering*. <https://doi.org/10.1007/s00202-019-00885-8>
- [23] Ahmadianroohbakhsh, Mohammadmehdi, Farzad Fahool, Mohammad Sadegh Saffari Pour, S. Farid F. Mojtahedi, Behnam Ghorbanirezaei, and Moncef L. Nehdi. 2023. "Approximating Helical Pile Pullout Resistance Using Metaheuristic-Enabled Fuzzy Hybrids" *Buildings* 13, no. 2: 347. <https://doi.org/10.3390/buildings13020347>
- [24] M. Veerachary, "Power tracking for nonlinear PV sources with coupled inductor SEPIC converter," *IEEE transactions on aerospace and electronic systems*, 41: 3 (2005): 1019- 1029.
- [25] I. H. Altas, A. M. Sharaf, "A photovoltaic array simulation model for matlab-simulink GUI environment," *Clean Electrical Power, 2007. ICCEP'07. International Conference on*. IEEE, 2007.
- [26] Angadi, S.; Yaragatti, U.R.; Suresh, Y.; Raju, A.B. System Parameter Based Performance Optimization of Solar PV Systems with Perturbation Based MPPT Algorithms. *Energies* **2021**, 14, 2007. <https://doi.org/10.3390/en14072007>

- [27] Sharma, D., and Purohit, G., 2012, "Advanced Perturbation and Observation (P&O) Based Maximum Power Point Tracking (MPPT) of a Solar Photo-Voltaic System" 2012 IEEE India International Conference on Power Electronics (IICPE), Delhi, India, Dec. 6–8.
- [28] Sweidan, T. O., and Widyan, M. S., 2017, "Perturbation and Observation as MPPT Algorithm Applied on the Transient Analysis of PV-Powered DC Series Motor," 8th International Renewable Energy Congress (IREC), Amman, Jordan, Mar. 21–23, pp. 1–6.
- [29] Kamran, M., Mudassar, M., Fazal, M. R., Asghar, M. U., Bilal, M., and Asghar, R., 2018, "Implementation of Improved Perturb & Observe MPPT Technique With Confined Search Space for Standalone Photovoltaic System," *J. King Saud Univ.—Eng. Sci.*, 32(1), pp. 432–441.
- [30] M. Nasir Uddin, Jeffrey Andrew-Cotter, Ifte Khairul Amin, "Performance Analysis of an Adaptive MPPT Control for a Grid-connected PV Solar System", 2022 *IEEE 1st Industrial Electronics Society Annual On-Line Conference (ONCON)*, pp.1-8, 2022.
- [31] Shantnu Sharma, Nitin Gupta, "An Overview on Topology and Control Techniques for Solar PV System", 2022 *1st International Conference on Sustainable Technology for Power and Energy Systems (STPES)*, pp.1-6, 2022.
- [32] Arif Indro Sultoni, Lukman Hanafi, Zaenal Panutup Aji, "Implementation of Fuzzy-PID Based MPPT for Stand Alone 1.75 kW PV System", 2020 *3rd International Seminar on Research of Information Technology and Intelligent Systems (ISRITI)*, pp.572-576, 2020.